

## SEMICONDUCTORS, ORGANIC

Semiconductors are materials that are characterized by resistivities intermediate between those of metals and of insulators. The study of organic semiconductors has grown from research on conductivity mechanisms and structure–property relationships in solids to include applications-based research on working semiconductor junction devices. Organic materials are now used in transistors, photochromic devices, and commercially viable light-emitting diodes, and the utility of organic semiconductors continues to increase.

The study of organic semiconductors and conductors is highly interdisciplinary, involving the fields of chemistry, solid-state physics, engineering, and biology. This article provides a treatment of the theoretical aspects of organic semiconductors as well as an overview of recent advances in the field and the uses of these materials based on their conductive and optical properties.

### 1. Theory

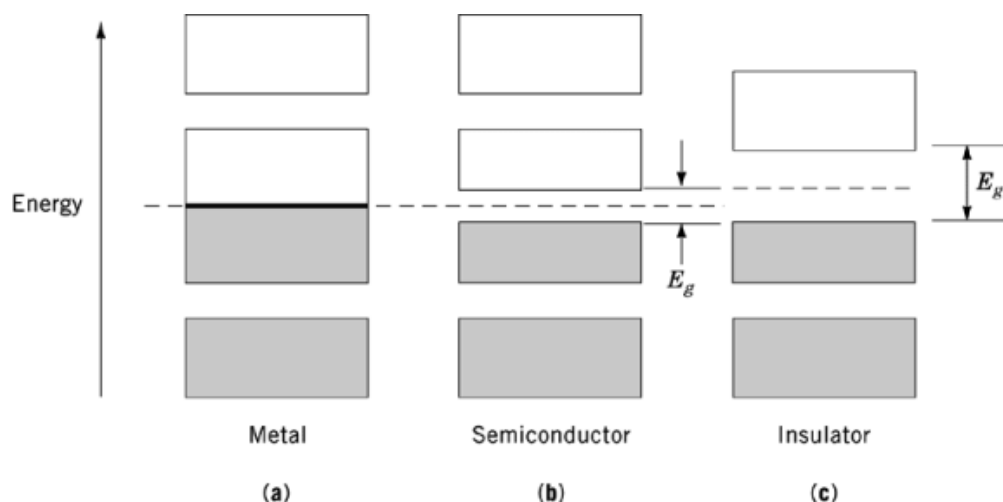
The theory of conduction in organic semiconductors conveniently begins with a discussion of bonding in extended solids, since the nature of conduction is intimately related to the extent of delocalization of orbitals in the material to be studied. For inorganic conducting solids, the orbital overlap of the atoms in the crystal lattice results in the atomic energy levels spreading out to form energy bands rather than discrete levels. These energy bands allow for motion of charge carriers over many lattice sites without interruption by trapping events. The interactions between molecules in a molecular organic solid similarly leads to the formation of energy bands, with the extent of interaction between molecules (the extent of overlap of interacting orbitals) determining the width of the bands.

The distinctions between metals, semiconductors, and insulators are based on the band structure of the materials as well as on the electron occupancy of these bands. Figure 1 is a diagram of energy bands and occupancies for various classes of solids. As can be seen in Figure 1, insulators have a filled band formed from the valence orbitals (a “valence band”) with a higher lying unfilled band formed from higher energy orbitals (the “conduction” band). The region between these has no allowed states, and the energy difference required to promote an electron from the valence to the conduction band is termed the band gap of the material. For an insulator, the band gap is large, typically  $>4$  eV. Since all of the levels of the valence band are filled, no electrons are able to carry current.

Metallic behavior is observed for those solids that have partially filled bands (Fig. 1b), that is, for materials that have their Fermi level within a band. Since the energy bands are delocalized throughout the crystal, electrons in partially filled bands are free to move in the presence of an electric field, and large conductivity results. Conduction in metals shows a decrease in conductivity at higher temperatures, since scattering mechanisms (lattice phonons, etc) are frozen out at lower temperatures, but become more important as the temperature is raised.

Semiconductors show thermally activated conductivity. The reason can be seen from Figure 1c. The band gap of a semiconductor is small relative to that of an insulator. Similar to insulators, pure intrinsic

## 2 SEMICONDUCTORS, ORGANIC



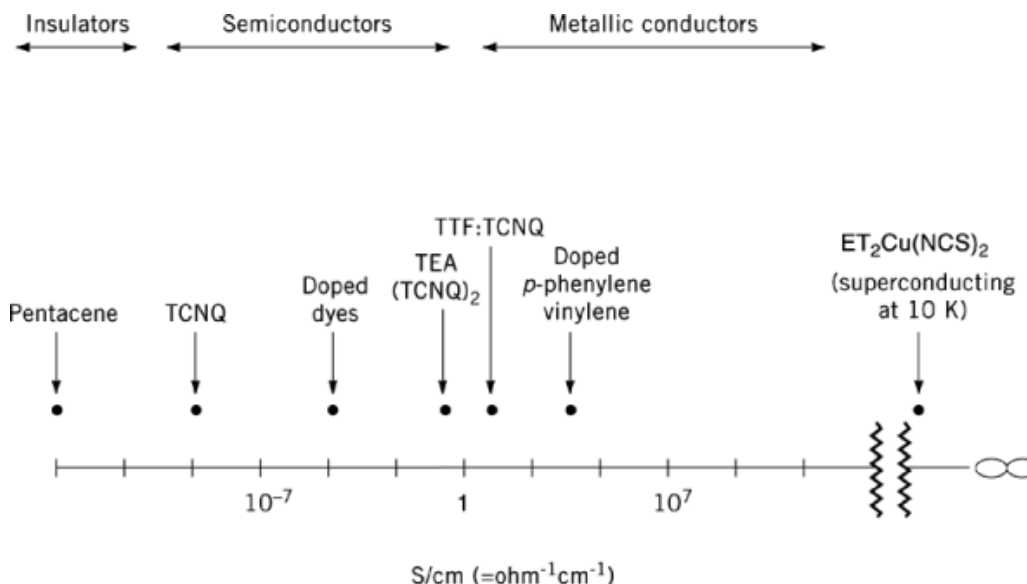
**Fig. 1.** Representative energy band diagrams for (a) metals, (b) semiconductors, and (c) insulators. The dashed line represents the Fermi Level, and the shaded areas represent filled states of the bands.  $E_g$  denotes the band gap of the material.

semiconductors have a filled valence band and unfilled conduction band. However, this is strictly true only at absolute zero. At higher temperatures, the energy of the surroundings  $kT$  can become large enough to thermally excite electrons from the valence to the conduction band, with the result that semiconductors have partially unfilled orbitals, giving rise to conduction. Typical band gaps for semiconductors are  $\sim 1 - 2$  eV. Increasing temperature causes increased electrical conductivity by providing more carriers in the conduction band.

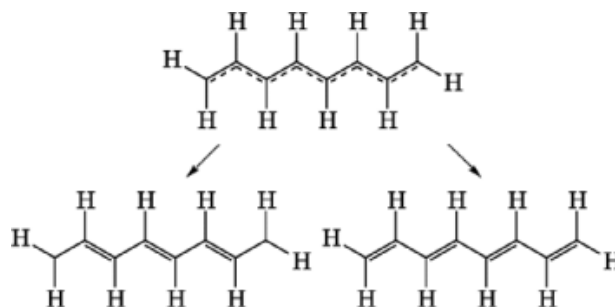
A variety of organic materials demonstrate reasonable conductivity, and a great deal of study has been devoted to conduction in organic materials. Initial study of conduction in organic materials was focused on molecular crystals (such as anthracene) that have weak intermolecular van der Waals interactions and low conductivities. However, the area of research has broadened and also includes charge-transfer compounds and polymeric materials. Research on new materials has led to synthesis of organic compounds with much larger conductivities than typical molecular crystals. Conducting and superconducting organic solids are now relatively commonplace. A listing of some compounds and associated conductivities are shown in Figure 2.

Certain one-dimensional, chain-like organic semiconductors are found to display metallic properties (decreasing conductivity with increasing temperature) above a certain temperature (1). The phase transition that occurs in these stacked materials is termed a metal-to-insulator transition and is the result of the highly anisotropic nature of these materials. A stack of equally spaced atoms or molecules is subject to a reorganization to a lower symmetry configuration. This reorganization, termed a Peierls distortion (2), is the condensed matter counterpart of the molecular Jahn-Teller distortion. The Peierls deformation results in pairing of molecules along the chain with the formation of short and long intermolecular spacings. This nuclear deformation causes changes in the electronic distribution of the lattice. The result of this redistribution is the opening of an energy gap at the Fermi level, with resulting semiconductivity. Reviews of Peierls distortions can be found in the literature (3).

A common example of the Peierls distortion is the linear polyene, polyacetylene. A simple molecular orbital approach would predict  $sp^2$  hybridization at each carbon and metallic behavior as a result of a half-filled delocalized  $\pi$ -orbital along the chain. Uniform bond lengths would be expected (as in benzene) as a result of the delocalization. However, a Peierls distortion leads to alternating single and double bonds (Fig. 3) and the opening up of a band gap. As a result, undoped polyacetylene is a semiconductor.



**Fig. 2.** Conductivity scale for different classes of organic materials.



**Fig. 3.** Representation of the Peierls distortion in *trans*-polyethylene.

Interaction of molecules to form charge-transfer complexes occurs via transfer of electron density from one molecule (an electron donor, D) to another (an electron acceptor, A), resulting in a partially ionic ground state. The amount of charge transfer is large when the ionization potential of the donor is low and the electron affinity of the acceptor is high. Orbital descriptions and experimental aspects of charge-transfer complexes have been studied extensively, especially for weak complexes (4). In a charge-transfer salt, the intermolecular interactions give rise to periodic arrays of donors and acceptors.

Typical charge-transfer salts form as stacks of planar D and A molecules, though the ratio of D:A need not be 1:1, as the interaction can be spread over more than two molecules. The amount of charge transfer ( $\delta$ ) per  $D^{\delta+}A^{\delta-}$  unit in the solid may be less than unity, with partial charges residing on the respective stacks. Interactions between stacks are usually weak, and the observed conductivity is, thus, anisotropic, with the preferred direction being along the stacking axis. Anion ( $A^-$ ) stacks result in electrical conductivity, while cation ( $D^+$ ) stacks conduct holes. Strongly bound charge-transfer systems are of primary interest for organic semiconducting applications. A listing of some common strong donors and acceptors is given in Table 1.

## 4 SEMICONDUCTORS, ORGANIC

**Table 1. Common Donor and Acceptor Molecules Used in Organic Semiconductor and Devices**

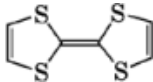
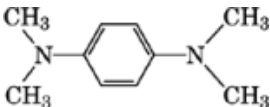
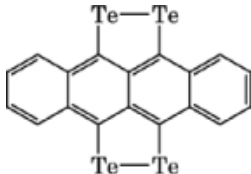
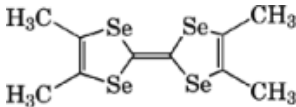
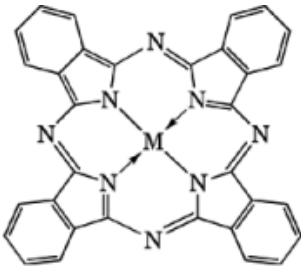
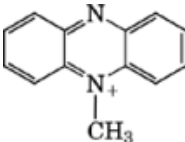
| Compound   | CAS Registry Number | Structure   |
|--|---------------------|---|
| <i>Donors</i>  |                     |   |
| 2,2',5,5'-tetrathiafulvalene (TTF)                               | [31366-25-3]        |    |
| <i>N,N,N',N'</i> -tetramethyl- <i>p</i> -phenylenediamine (TMPD) | [100-22-1]          |    |
| 5,6;11,12-tetratellurotetracene                                  | [64479-92-1]        |    |
| 3,3',4,4'-tetramethyl-2,2',5,5'-tetraselenafulvalene (TMTSF)     | [55259-49-9]        |  |
| phthalocyanines (PC), M = Cu                                     | [147-14-8]          |  |
| <i>N</i> -methylphenazinium (NMP)                                | [7432-06-6]         |  |

Table 1. *Continued*

| Compound  | CAS Registry Number | Structure |
|---|---------------------|-----------|
| <i>Acceptors</i>                                      |                     |           |
| 7,7,8,8-tetracyanoquinodimethane                      | [1518-16-7]         |           |
| tetracyanoethylene (TCNE)                             | [670-54-2]          |           |
| 9,9,10,10-tetracyano-2,6-naph-thylenedimethane (TNAP) | [6251-01-4]         |           |
| chloranil   | [118-75-2]          |           |
| trinitrofluorenone (TNF)                              | [129-79-3]          |           |

Some common single-carrier semiconducting salts are tetracyanoquinodimethane (TCNQ) radicals with alkali or other cations. The study of semiconductivity in these materials led to synthesis of more highly conductive charge-transfer salts based on the strong donor tetrathiafulvalene (TTF) with halogen or other acceptors. Organic materials have been developed with even larger conductivity and superconductivity above liquid helium temperatures.

## 6 SEMICONDUCTORS, ORGANIC

### 2. Properties

#### 2.1. Physical Properties: Electrical

Electrical properties have been the main focus of study of organic semiconductors, and conductivity studies on organic materials have led to the development of materials with extremely low resistivities and large anisotropies. A discussion of conductivity behaviors for various classes of compounds follows.

##### 2.1.1. Charge-Transfer Salts

Most organic molecular crystals have only weak interactions between molecular units and have resulting low conductivities, with  $S < 10^{-10} \Omega^{-1} \text{cm}^{-1}$ . Charge-transfer solids tend to have higher conductivities than the molecular compounds from which they are composed, and semiconducting charge-transfer salts of TCNQ were first synthesized in the early 1960s. The simple metal-ion radical salts of the composition  $M^+(\text{TCNQ})^-$  have conductivities of  $\sim 10^{-9} - 10^{-4} \Omega^{-1} \text{cm}^{-1}$  at room temperature, intermediate between conductivity values for insulators and typical metals. A variety of other systems show thermally activated conductivity in the range  $10^{-10} - 1 \Omega^{-1} \text{cm}^{-1}$ , including phthalocyanines and chloranil or tetracyanoethylene-based charge-transfer complexes. Conductivity in these semiconductive compounds obeys an Arrhenius expression:

$$\sigma = Ae^{-\Delta E/kT}$$

where  $A$  is a preexponential factor,  $k$  is Boltzmann's constant and  $\Delta E$  is the activation energy for the thermally activated conductivity.

Proposed conductivity mechanisms and the importance of band motion vs hopping motion in semiconducting organic solids have generated a great deal of controversy. However, it is plausible that for many organic molecular semiconducting materials, the description of the conductivity lies somewhere between the extremes of localized hopping and delocalized band models (5).

The highly conductive class of solids based on TTF-TCNQ have less than complete charge transfer ( $\sim 0.6$  electrons/unit for TTF-TCNQ) and display metallic behavior above a certain temperature. However, these solids undergo a metal-to-insulator transition and behave as organic semiconductors at lower temperatures. The change from a metallic to semiconducting state in these chain-like one-dimensional (1D) systems is a result of a Peierls instability. Although for true one-dimensional systems this transition should take place at 0 Kelvin, interchain interactions lead to effective non-1D behavior and inhibit the onset of the transition (6).

The temperature of the metal-to-insulator transition in TTF-TCNQ is 53 K. For systems with increased interchain coupling, the transition temperature for the onset of metallic conduction increases roughly as the square of the interaction between the chains. This behavior is true as long as the coupling between chains remains relatively weak. For compounds with strong interactions between stacks, the material loses its quasi-1D behavior. Thus, the Peierls distortion does not occur even at low temperatures, and the materials remain conductive.

The temperature range of metallic conductivity in organic materials can sometimes be increased by compaction of the compound under large pressures. For example, bis(tetramethyl tetraselenafulvalenium) hexafluorophosphate ( $(\text{TMTSF})_2\text{-PF}_6$ ) undergoes a metal-to-insulator transition at 12 K at atmospheric pressure. Under high pressures, however, the material stays conducting to low temperatures and goes superconducting at 0.9 K (7). A variety of organic-based materials have now been developed that have strong interchain interactions and possess superconductivity at low temperatures. Examples include bis(tetramethyl tetraselenafulvanenium) perchlorate  $(\text{TMTSF})_2\text{ClO}_4$  and compounds based on the donor molecule bis(ethylenedithio)tetrathiafulvalene (BEDT-TTF) with a variety of inorganic and organic anions (8).

### 2.1.2. Polymers

The use of polymers in semiconducting applications is growing rapidly. In the undoped form, most of these  $\pi$ -conjugated systems are semiconducting, with a small band gap separating filled valence and conduction bands. A listing of polymers commonly used in semiconducting applications is given in Table 2. The dark (nonphotoinduced) conductivity of these systems is typically low and increases with increasing temperature, as a result of thermalization of charge carriers. Doping the material leads to large increases in conductivity, with increases of several orders of magnitude possible. Doping removes electrons from the valence band or adds them to the conduction band. However, the charges are not delocalized along the polymer chain. An extra electron in the conduction band, for example, becomes localized as a result of a local geometry change caused by the excess charge. The result of the charge localization is termed a polaron, which as a result of the local energy minimum gives a state in the bandgap of the material. Conduction can then occur by motion of the polaron through the chain.

Conductivities of polymers of technological interest such as polypyrrole and polythiophene are typically  $\sim 100 \Omega^{-1} \text{cm}^{-1}$  in the doped state, and the conductivity can be tuned by reversibly doping and undoping the polymer. Derivatives of these and other polymers have achieved even higher conductivities.

One-dimensional polymers such as polyacetylene which have degenerate ground states are special cases. Conduction in polyacetylene has been extensively studied (9). The nature of conduction in pure, *trans*-polyacetylene is a result of the alternating single bond–double bond structure that results from the Peierls instability. The energy of the system is the same if the alternating pattern of the bonds is reversed. Conductivity has been described for this system in terms of solitons (mobile kinks in the polymer chain that link alternating bond patterns), excitations that are unique to systems with degenerate ground states (10, 11). These neutral solitons are mobile, and extend over several bond lengths along the chain. As usually prepared, undoped polyacetylene has *p*-type conductivity as a result of acceptor impurities in the material. The conductivity increases with doping, reaching a plateau value at high doping levels (12). Highly doped *trans*-polyacetylene can display conductivities as high as  $10^5 \Omega^{-1} \text{cm}^{-1}$ .

## 2.2. Optical Properties

### 2.2.1. Charge-Transfer Salts

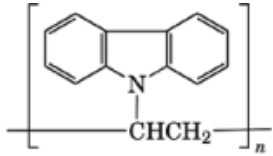
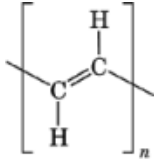
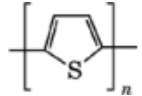

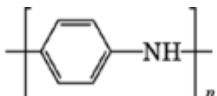
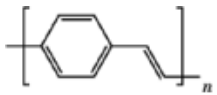
New strong absorbance bands (charge-transfer bands) are often observed in spectra of donor–acceptor solids. These bands are the result of excitation from a ground state that is predominantly donor in character to an excited state that resides mainly on the acceptor. For a given acceptor, the frequency of this band varies linearly (over a small range) with the ionization potential of the donor molecule. This absorption band can occur at lower energy than absorptions of the isolated D and A molecules, and is often in the infrared region. By a suitable choice of donor and acceptor, it is possible to tune the frequency of this absorption band (and the associated fluorescence) throughout the visible region. For compounds such as the simple charge-transfer salts of TCNQ (formula  $\text{M}^+\text{TCNQ}^-$ ) the charge transfer is complete, and these salts in solution exhibit spectra characteristic of the anion. In the solid state, an additional absorption band is observed as a result of charge transfer between adjacent  $\text{TCNQ}^-$  molecules: one acting as a  $\pi$ -donor and the other as a  $\pi$ -acceptor. Highly conducting salts such as those of the formula  $\text{M}^+\text{TCNQ}^-(\text{TCNQ})$  have less than a complete negative charge per TCNQ molecule in the stack. These compounds exhibit an additional transition as a result of promotion of an electron from an anionic to neutral TCNQ site.

### 2.2.2. Polymers

Polymers used in semiconducting applications such as light-emitting diode displays are  $\pi$ -conjugated systems with small band gaps of 1–3.5 eV. In the undoped state they give strong  $\pi-\pi^*$  absorption bands in the visible or ultraviolet region, corresponding to transitions from the valence band to the conduction band levels. By tailoring

## 8 SEMICONDUCTORS, ORGANIC

**Table 2. Representative Polymers Used for Organic Semiconductors and Metals**

| Compound                                  | CAS Registry Number | Structure   |
|---|---------------------|---|
| <i>Polymers</i>                           |                     |   |
| polyvinylcarbazole (PVK)                  | [25067-59-8]        |    |
| <i>trans</i> -polyacetylene               | [25067-58-7]        |    |
| polythiophene                             | [25233-34-5]        |    |
| poly( <i>p</i> -phenylene)                | [25190-62-9]        |  |
| polyaniline (PANI)                        | [25233-30-1]        |  |
| poly( <i>p</i> -phenylene vinylene) (PPV) | [26009-24-5]        |  |

the nature of the electron-donating and withdrawing substituents on the polymer backbone, absorbance and the resulting emission spectra can be shifted throughout the visible region. Conformational changes due to heating can drastically shift the absorption, suggesting possible uses as molecular switches.

Doping of the polymers brings about absorbances in addition to the main bandgap transition. These absorbances occur at lower energies, and grow in at the expense of the band-to-band transition. The new absorbances are due to transitions between states that lie in the band gap of the material (13). These midgap states are typically polaron states that arise due to the injected charge-carriers being localized by lattice distortions. As the doping levels are increased, absorption at lower energies continues to increase and the



original band edge becomes obscured. At high doping levels the polymers show absorption throughout the ir and visible, consistent with metallic behavior.

### 2.3. Chemical Properties: Electrochemistry

Since charge-transfer and mobility of carriers are important features for organic semiconductors and devices, the energies of the highest occupied molecular orbital (HOMO) and lowest unoccupied molecular orbital (LUMO) are of interest. The energies of these levels are related to the efficiency of charge injection into a material as well as the degree of charge-transfer between donors and acceptors. Electrochemical measurements provide a convenient means for determining HOMO and LUMO levels by measuring the potentials required for oxidation and reduction of the material, respectively. Redox potentials also provide a quick method for checking energy gap values obtained from conductivity measurements.

Electron donor molecules are oxidized in solution easily. For example,  $E_{1/2}^{ox}$  for TTF is 0.33V vs SCE in acetonitrile. Similarly, electron acceptors such as TCNQ are reduced easily. TCNQ exhibits a reduction wave at  $E_{1/2}^{red} = 0.06V$  vs SCE in acetonitrile. The redox potentials can be adjusted by derivatizing the donor and acceptor molecules, and this tuning of HOMO and LUMO levels can be used to tailor charge-transfer and conductivity properties of the material. Knowledge of HOMO and LUMO levels can also be used to choose materials for efficient charge injection from metallic electrodes.

Reversible oxidation and reduction of polymers is commonly used to increase conductivity in these systems. Ions from the electrolyte are usually incorporated into the polymer as part of this process (see Electrically conducting polymers).

### 2.4. Stability

#### 2.4.1. Thermal Stability

The materials used in organic semiconducting applications are thermally labile upon exposure to high temperatures. For example, many of the compounds used in fabrication of organic light-emitting diodes (LEDs) are vapor deposited by resistive heating at relatively low temperatures in vacuum. Compounds such as the hole transporter *N,N'*-biphenyl-*N,N'*-bis(3-methylphenyl)-1,1' biphenyl-4,4' diamine (TPD) have glass-transition temperatures in the range of 150°C.

As a result of the organic nature of the materials, chemical oxidation is a problem when heating in atmosphere. For example, TTF melts at 119°C, with the formation of sulfoxides as a result of oxidation of the sulfur atoms in the molecule (14). Polymeric compounds can also oxidize at low temperatures. Polyacetylene is degraded at room temperature by atmospheric oxygen and water vapor. Although other conjugated polymers are typically more thermally stable, most exhibit degradation and decreased conductivity after heating in atmosphere.

#### 2.4.2. Photostability and Atmospheric Stability

The presence of oxygen and water vapor has a profound effect upon the photostability of many organic semiconducting materials. For example, singlet oxygen has been found to be a highly reactive intermediate in the photooxidation of poly(phenylene vinylene) derivatives (15). Oxygen and water vapor have also been implicated in dark spot formation in the degradation of light-emitting diodes. As a result, performance lifetimes of these devices can be significantly prolonged by packaging under inert atmosphere. An exception to the general behavior of organic semiconducting systems is observed for *p-n* solar cells fabricated with the donor chloroaluminum phthalocyanine. These cells exhibit improved performance after exposure to water and oxygen, due to formation of a crystalline hydrate (16). This provides further evidence for the need for control over impurity and humidity levels during device production.

### 3. Structure

A discussion of structure in organic semiconductors includes chemical structure of individual molecules or unit cells, as well as three-dimensional structure of the bulk material. The structure of individual molecules can be tailored by synthetic methods, with molecules designed for specific applications. For example, rigid, planar structures are often used for dyes in photovoltaics, since this increases exciton mobility. Molecular packing and the structure of thin films can be dependent upon the method of fabrication and the structure of individual units. The nature of molecular and polymeric thin films for semiconducting applications ranges from highly crystalline to amorphous. Challenges ahead are to design better adhesion between organic films and substrates. Better interfacing and orientation are needed for many applications, since these can influence charge injection and transport. Though the structure of organic semiconductors is wide ranging, some common classes are discussed below.

#### 3.1. Single-Stack Acceptor

Simple charge-transfer salts formed from the planar acceptor TCNQ have a stacked arrangement with the TCNQ<sup>-</sup> units facing each other (intermolecular distances of ca 0.3 nm (~3). Complex salts of TCNQ such as TEA(TCNQ)<sub>2</sub> consist of stacks of parallel TCNQ molecules, with cation sites between the stacks (17). The interatomic distance between TCNQ units is not always uniform in these salts, and formation of TCNQ dimers (as in TEA(TCNQ)<sub>2</sub>) and trimers (as in Cs<sub>2</sub>(TCNQ)<sub>3</sub>) can lead to complex crystal structures for the chainlike salts.

#### 3.2. Single-Stack Donor

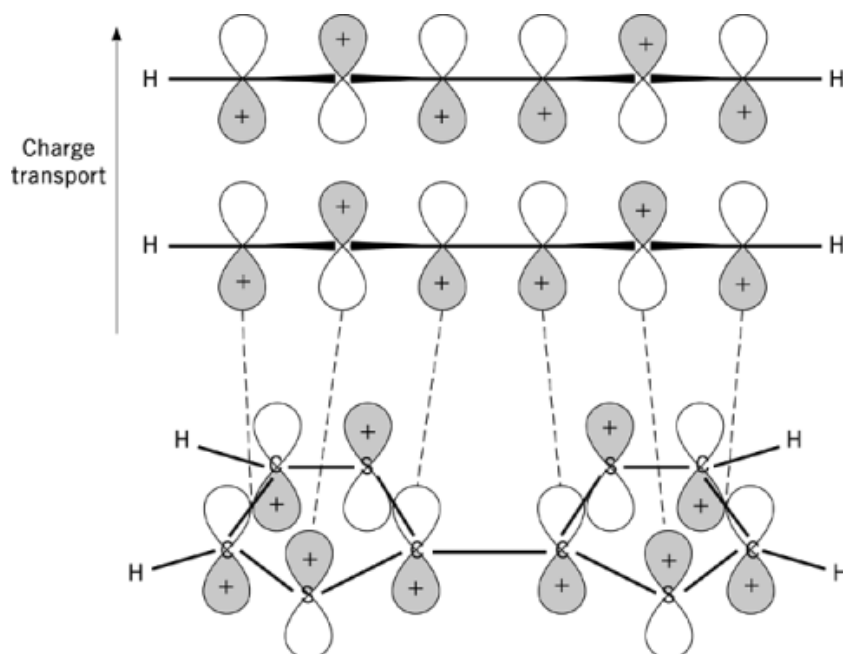
Ion-radical salts can also be formed from electron donors such as tetrathiafulvalene (TTF) or TMPD (*N,N,N',N'*-tetramethyl-*p*-phenylene diamine) with inorganic acceptors such as halogens. The resulting structure of compounds such as TTF(A)<sub>x</sub> (A = acceptor) is a linear chain of parallel stacked TTF molecules. The TTF molecules are registered directly above one another, with anions residing in sites between the TTF chains. Unlike the situation found for the TCNQ salts, the TTF molecules in these solids are equally spaced along the chain. Substantial  $\pi$ -overlap exists between the TTF molecules in the chain, providing for conduction along the stacking direction (Fig. 4).

A large family of compounds is based on combination of TTF-type donors and TCNQ-type acceptors. The resulting D<sup>δ+</sup>A<sup>δ-</sup> solids form segregated stacks of D and A molecules with uniform spacings along the stacks. Molecules are tilted with respect to the stacking axis, and the  $\pi$ -overlap of the molecules on each chain results in the formation of bands and large conductivity along the stacking direction.

A number of other donor-acceptor molecular solids such as TMPD<sup>δ+</sup> – TCNQ<sup>δ-</sup> or TMPD<sup>δ+</sup>chloranil<sup>δ-</sup> crystallize as mixed stacks of alternating D and A molecules. These compounds typically have much higher resistivities than the segregated salts because the alternating -DADA- sequence leaves no continuous channel for conduction.

#### 3.3. Polymers

The individual units in a polymer are well-defined, but bulk polymer usually lacks the periodic structure characteristic of inorganic or small molecule crystalline solids. The structure of semiconducting and conducting polymers is determined by the units of the polymer backbone as well as pendant side-groups (18). Typical conducting polymers are conjugated systems that provide for motion of the electrons through the  $\pi$ -system, and both linear chain (poly-acetylenes) and aryl chain poly(*p*-phenylene) polymers are commonly used. As chain length increases during polymer growth, the long-chain polymers become insoluble and precipitate out



**Fig. 4.** Orbital overlap for conduction molecular orbitals and molecular stacking in tetrathiafulvalene (TTF).

during synthesis. The chain length in polymeric solids is thus, influenced by the nature of the solvent and the synthetic process. Although most polymers are fairly amorphous, chemical substitution has been used to design self-assembled oligomeric films with highly ordered structures (19). Film morphology for linear chain polymers can be affected by stretching of the film to orient the chains, resulting in higher crystallinity. The morphology of electrochemically grown conducting polymer thin films has also been shown to be dependent on the nature of the substrate (20).

The conducting polymer poly(sulfur nitride) is unusual in that it is crystalline, consisting of chains of sulfur and nitrogen packed in parallel. Individual chains are planar with alternating cis-trans conformation along the chain, and the interaction with neighboring chains leads to a highly ordered matrix.

Although its use as a transparent electrode in diodes has made it one of the most useful of the conductive polymers, the intractable nature of the material made the structure of polyaniline difficult to determine. Recent studies of polyphenyleneamineimines have conclusively shown that the structure of PANI is an exclusively para-linked system (21).

## 4. Synthesis and Manufacture

### 4.1. Donors

Common selenium and sulfur-containing donors such as tetrathiafulvalene [31366-25-3], tetramethyltetrasele-nafulvalene [55259-49-9], and bis-(ethylenedithio)tetrathiafulvalene [66946-47-3] are commercially available, as are other common donors such as tetramethyl-*p*-phenylenediamine [100-22-1]. Tellurium-containing donors can be prepared using a variety of synthetic routes. Tetratellurafulvalene, for example, is prepared in good yield using tin-lithium exchange (22) (Fig. 5).

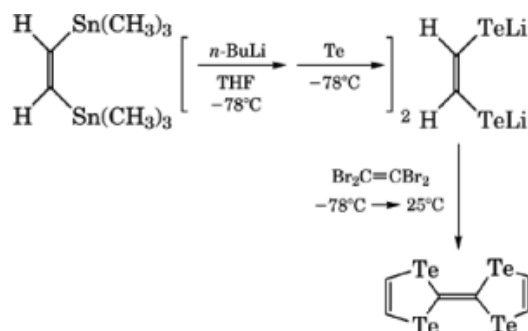


Fig. 5. Synthesis of the common donor tetratellurafulvalene.

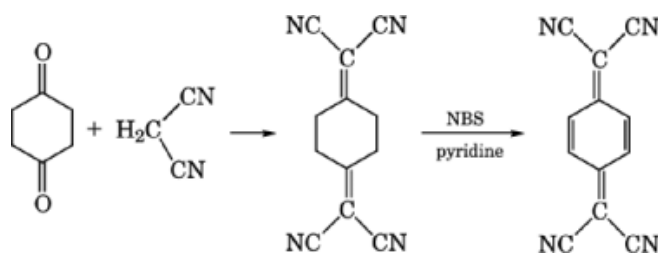


Fig. 6. Synthesis of the acceptor molecule tetracyanoquinodimethane (TCNQ).

#### 4.2. Acceptors

Most common acceptor molecules such as tetracyanoethylene or tetracyanoquinodimethane are commercially available. However, TCNQ can be synthesized in high yield by a two-step synthesis involving a condensation of malonitrile with 1,4-cyclohexanedione followed by treatment with an oxidizing agent such as bromine or *N*-bromosuccinimide in pyridine solvent (23) (Fig. 6).

#### 4.3. Charge-Transfer Salts

Most charge-transfer salts can be prepared by direct mixing of donors and acceptors in solution. Semiconducting salts of TCNQ have been prepared with a variety of both organic and inorganic counterions. Simple salts of the type  $M^+TCNQ^-$  can be obtained by direct reaction of a metal such as copper or silver with TCNQ in solution. Solutions of metal iodides can be used in place of the metals, and precipitation of the TCNQ salt occur directly (24).

More highly conducting TCNQ salts of the form  $M^+(TCNQ)(TCNQ^-)$  are also easily synthesized, where  $M^+$  can be any one of a variety of organic cations. These salts can be prepared by a number of different methods, though a general method involves mixing of a simple salt with TCNQ in solution. The precipitated salt can then be obtained by filtration.

Compounds containing the donor and acceptor moieties on the same molecule have also been prepared. A class of these compounds contains the D and A parts separated by sulfur atoms (a D- $\sigma$ -A linkage), with the acceptor portion based on the TCNQ structure (25). Syntheses of these molecules can provide for the design of substituent groups to tailor packing and conducting properties in the solid state. Linkages of this D- $\sigma$ -A type have garnered interest for possible use as unimolecular rectifiers (26).

#### 4.4. Polymers

The  $\pi$ -conjugated polymers used in semiconducting applications are usually insulating, with semiconducting or metallic properties induced by doping (see Electrically conductive polymers). Most of the polymers of this type can be prepared by standard methods. The increasing use of polymers in devices in the last decade has led to a great deal of study to improve the processability of thin films of commonly used polymers.

Polyacetylene is the most studied of all of the polymers used in semiconducting applications. Early syntheses of polyacetylene were based on direct polymerization of acetylene using a Ziegler-Natta catalyst (usually titanium tetrabutoxide and triethylammonium) coated onto a glass substrate (27). The resulting polyacetylene films from these direct polymerizations were highly crystalline, insoluble, unstable with respect to atmosphere, and of low tensile strength. Other preparations from polymerization of acetylene have resulted in better film properties and higher conductivities; however, the films are not easily processible. To improve processibility and to generate new morphologies of polyacetylene that possess superior properties, precursor methods have been used (28). Polyacetylene has been prepared by ring-opening polymerization of polybenzvalene (29) as well as by polymerization involving addition of catalysts to 1,3,5,7 cyclooctatetraene (COT) (30). A variety of derivatives of polyacetylene can be generated with substituted precursor derivatives.

Polyaniline (PANI) can be formed by electrochemical oxidation of aniline in aqueous acid, or by polymerization of aniline using an aqueous solution of ammonium thiosulfate and hydrochloric acid. This polymer is finding increasing use as a “transparent electrode” in semiconducting devices. To improve processibility, a large number of substituted polyanilines have been prepared. The sulfonated form of PANI is water soluble, and can be prepared by treatment of PANI with fuming sulfuric acid (31). A variety of other soluble substituted *N*-alkylsulfonic acid self-doped derivatives have been synthesized that possess moderate conductivity and allow facile preparation of spincoated thin films (32).

Polythiophene can be synthesized by electrochemical polymerization or chemical oxidation of the monomer. A large number of substituted polythiophenes have been prepared, with the properties of the polymer depending on the nature of the substituent group. Oligomers of polythiophene such as ( $\alpha$ -sexithienyl thiophene) can be prepared by oxidative linking of smaller thiophene units (33). These oligomers can be sublimed in vacuum to create polymer thin films for use in organic-based transistors.

### 5. Health and Safety Factors

Selenium is an essential element and is beneficial at low concentrations, serving as an antioxidant. Lack of selenium affects thyroid function, and selenium deficiencies have been linked to Keshan Disease (34). Selenium at high levels, however, is toxic. Hydrogen selenide (which is used in semiconductor manufacturing) is extremely toxic, affecting the mucous membranes and respiratory system. However, the toxicity of most organoselenium compounds used as donor compounds for organic semiconductors is not well studied.

Tellurium is not an essential element, and tellurium compounds are in general more toxic than their selenium counterparts. Metallic tellurium is known to have a teratogenic effect in rats, though no studies have been done on the toxicity of tellurium donor compounds (35).

The common acceptor molecule tetracyanoethylene is a poison, and sublimes at relatively low temperature (120°C). The toxicological effects of most cyano-type acceptors have not been fully investigated.

### 6. Uses

The performance of early organic semiconductor-based devices was far below that of their Si-based counterparts. In addition, the poor stability and reliability of many organic-based devices slowed their practical use.

However, many problems have been overcome and these devices are becoming increasingly in a variety of applications. Organic semiconductors offer many advantages over inorganic-based materials for use in electronic and optoelectronic devices. Among the advantages are the possibility of tailoring properties through synthetic chemical modifications, the relative ease of generating large-area films, and low cost device manufacture. The following is a summary of some current uses and areas of research for potential applications.

### 6.1. Diodes

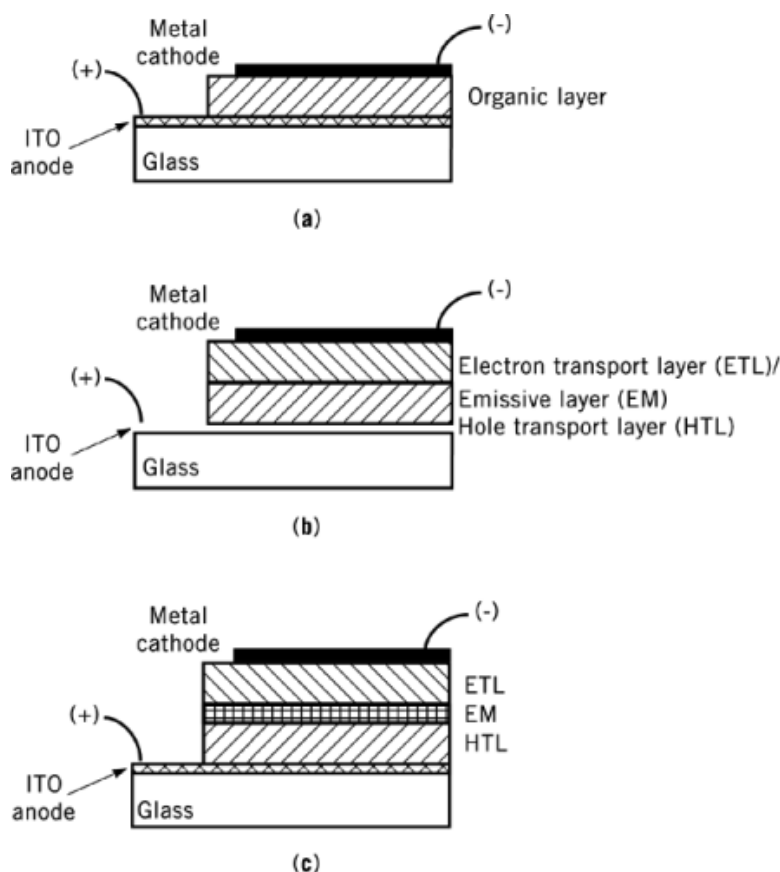
The first reports of electroluminescence (EL) from organic materials appeared in the 1960s (36–38), but it was not until 1987 that Tang and VanSlyke reported an Organic Light Emitting Diode (OLED) device with reasonable efficiency (39). The key to preparing an efficient device is to use a number of different metal–organic or organic thin-films materials, each serving a different function in the working device. Early devices consisted of two organic layers, one a tertiary amine and the other an aluminum coordination complex (aluminum-tris-8-hydroxyquinoline), the latter of which is responsible for bright green light emission. Over the last several years research on these novel devices has led to new organic and metal–organic materials with emission that covers the entire visible spectrum (40–46). Quantum efficiencies for these devices are comparable to LEDs based on inorganic semiconductors, typically ranging from 1–2.5% (photons/electrons) (41, 47). OLEDs can achieve very high brightnesses, of greater than 15,000 cd/m<sup>2</sup> (43, 48) and have operational lifetimes greater than 10,000 hours when driven at video brightness (100 cd/m<sup>2</sup>) (49).

OLEDs are based on amorphous (glassy) organic films, which can be deposited on virtually any substrate, ranging from rigid supports such as glass or silicon to highly flexible polymer supports (50). This is in contrast to inorganic LEDs, which require crystalline substrates for epitaxial growth of the active materials. An additional feature of OLEDs is that the organic layers are very thin (ca 50–100 nm, 500–1000 Å), and combined with large Franck-Condon shift between absorption and emission, makes them transparent to their own emission (51, 52). This transparency may open the door to novel display architectures and applications. Taking these qualities together it is clear that OLEDs have unique characteristics as compared with other potential flat panel display (FPD) technologies. Although technical obstacles must be overcome, OLEDs have potential for certain display applications. This section is an overview of device structure and performance.

#### 6.1.1. Device Structure and Operation

Efficient generation of electroluminescence in OLEDs depends on several factors. Injection of carriers (electrons and holes) from the respective electrodes, transport of carriers through the device, and radiative recombination of carriers must all be optimized. A simple OLED consisting of a thin organic or metal–organic film between an indium–tin–oxide (ITO) anode and a metal cathode is shown in Figure 7a. When a potential is applied to the device, the material is oxidized at the anode and reduced at the cathode, leading to the injection of holes and electrons, respectively, into the thin film. The holes and electrons injected into the thin film drift in the presence of the applied field via a hopping mechanism until they are removed at the opposite electrode or encounter an oppositely charged carrier within the film. In the latter case, electron–hole recombination results in the formation of an exciton and resultant emission of light.

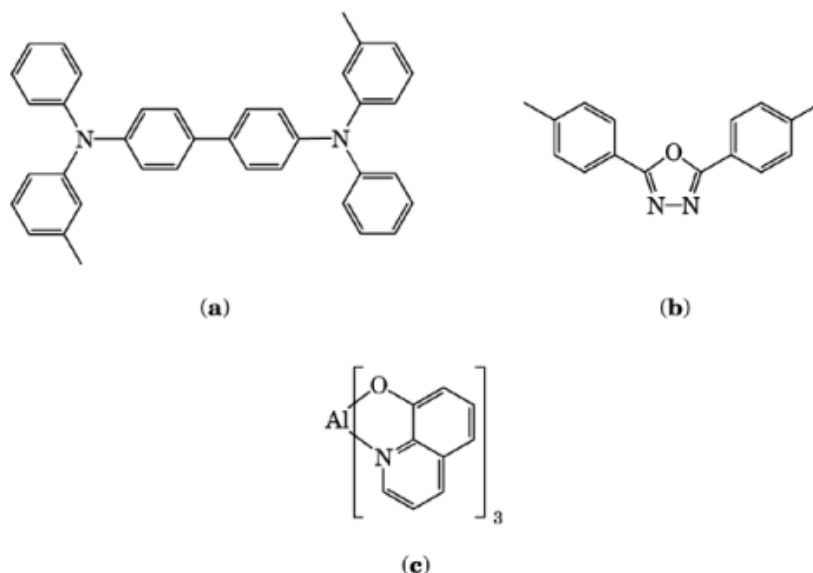
Single layer OLEDs have been fabricated with a variety of emitter molecules and conjugated polymers such as poly(phenylene vinylene) (PPV). These single-layer devices are typically not very efficient. To ensure high injection efficiency of both electrons and holes, multiple organic layers are used with each layer optimized for its particular role as a carrier injector or light emitter. The first efficient EL device was a single heterostructure (Fig. 7b), with a tertiary amine hole–transport layer (HTL) and an aluminum complex serving both as the electron-transport layer (ETL) and emissive material (EM) (39). In this device, the preferred conductivity of holes in the HTL and electrons in the ETL leads to a build up of carriers at the HTL–ETL interface. The excitons are formed at the interface, however, and hence are not spatially confined. As a result, it is important that the thickness of the ETL–EM layer emitter be chosen such that the majority of the excitons radiatively



**Fig. 7.** Schematic of light emitting diodes: (a) single-layer device (b) single heterostructure (c) double heterostructure.

decay prior to reaching the adjacent electrode. The choice of ITO for the anode, and a suitable metal as the cathodes is based on the energies of the filled and vacant states of the organic materials relative to the work functions of these contacts. ITO is well matched to inject holes into the HTL HOMO, and low work function metals such as Mg, Al, and Ca can inject electrons into the ETL LUMO. Under forward bias (ITO positive) the injection of holes into the HTL and electrons into the ETL occurs at low ( $\sim 5$  V) potentials, while reversing the bias requires much higher potentials to inject the same current density. Hence, OLEDs show strongly rectifying current–voltage behavior.

An example “double heterostructure” OLED shown in Figure 7c uses an ITO coated glass substrate, upon which a hole transporting layer, typically composed of a tertiary amine (eg, *N,N'*-biphenyl-*N,N'*-bis(3-methylphenyl)-1,1'-biphenyl-4,4'-diamine, abbreviated TPD), a thin film of an emissive material such as aluminum-8-hydroxyquinoline ( $\text{Alq}_3$ ) and an electron-transporting layer (often an oxadiazole derivative) are sequentially deposited in vacuum (Fig. 8). This molecular multilayer is then capped with a cathode to complete the device. The HTL and ETL have high mobilities for holes and electrons, respectively, but very low mobilities for the oppositely charged carrier. When an electric field is applied to this device, holes will move through the HTL to the HTL–EM interface and electrons will move through the ETL to the ETL–EM interface. These carriers then form a bound state exciton, and subsequently recombine in the EM, leading to efficient light



**Fig. 8.** Structures of (a) hole transporter molecule *N,N'*-biphenyl-*N,N'*-bis(3-methylphenyl)-1,1'-biphenyl-4,4'-diamine (TPD); (b) an oxidiazole derivative; and (c) the common emitter, 8-hydroxyquinoline.

emission. For efficient recombination at the emitter site, the emitter molecule should have a HOMO higher than that of the HTL and a LUMO lower than that of the ETL (53).

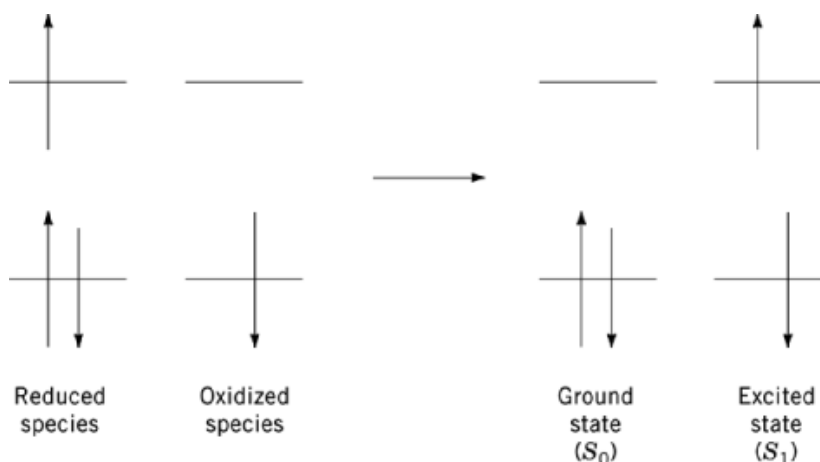
The picture presented above for confinement of the excitons within the device is for the EM layer sandwiched between the HTL and ETL. The EM need not be a discrete layer in the OLED, however, for exciton confinement to occur. Alternatively, the EM can consist of a luminescent molecule doped ( $\sim 1\%$ ) into a polymeric or molecular host material (40, 41, 54, 55). So long as the energy gap (or band gap) of the host is higher than that of the EM dopant, excitons will be effectively trapped or confined on the dopant molecules leading to improved EL efficiency. An example of such a dopant-based device involves tetraphenylporphyrin doped into the Alq<sub>3</sub> layer of a TPD–Alq<sub>3</sub> OLED. Even at the dopant concentrations typically used (0.5–1%), the luminescence is entirely due to the tetraphenylporphyrin (54). A wide range of fluorescent and laser dyes have been developed with emission colors spanning the visible spectrum. These materials have very high luminescent quantum efficiencies in dilute solution, making them excellent candidates as emitter dopants in OLEDs, and indeed many have already been incorporated into efficient dopant-based OLEDs.

It has recently been shown that in some cases, the HTL and ETL materials do not need to be segregated into individual layers to achieve high device efficiency. For example, a homogeneous blend can be prepared with a polymeric hole transport (HT) material, and either a molecular or polymeric light emitter and electron transport (ET) material (53, 56–61). An OLED prepared in this manner consists of a single organic film sandwiched between an ITO anode and a metal cathode. As in conventional devices, holes are injected from ITO and electrons from the metal cathode, with recombination occurring within the thin polymer film. Polymers and monomeric metal complexes have been used successfully in these blended devices to give colors that span the visible spectrum, with external quantum efficiencies  $> 1\%$  (56, 57).

### 6.1.2. Emission

Generally, the shape of the electroluminescent spectrum is identical to that observed in photoluminescence. The reason for this can be seen by considering molecular LEDs. For closed shell molecules, the ground state  $S_0$





**Fig. 9.** Representation of exciton formation in molecular LEDs.

has two electrons in the highest occupied molecular orbital (HOMO), and a completely vacant orbital for the lowest unoccupied molecular orbital (LUMO). In the  $S_1$  excited state, both the HOMO and LUMO are singly occupied. Consider a molecular OLED with a thin organic film between an ITO anode and metal cathode. Since these films consist of weakly interacting molecules, the oxidized and reduced versions of the molecule correspond to the case where holes and electrons, respectively, are located at that molecular site. The holes and electrons move through the device, towards opposite electrodes. When the electron and hole combine, electron transfer from the reduced molecule (electron carrier) to the oxidized molecule (hole carrier) occurs, leading to a molecule to its ground electronic state,  $S_0$ , and an adjacent one to the  $S_1$  or Frenkel state (Fig. 9). The  $S_1$  state then relaxes exactly as for photoluminescence. The close relationship between electroluminescence and photoluminescence is not surprising since the emission comes from the same excited state (or Frenkel exciton) in both processes. It should be noted that low levels of impurities can cause quenching of the emission or emission from the impurity due to exciton trapping. As a result, materials used in OLEDs are typically purified by repeated sublimation.

Single emitter devices can be made in a variety of colors, with good efficiency. The color of the device emission can be altered in several ways. One of the most common ways is the use of dopants, as mentioned earlier. Förster energy transfer from the host to the dopant is maximized when the overlap of the host emission spectrum and the dopant absorption spectrum is favorable. By the use of suitable dopants, emission can be tuned and narrowed. In both molecular and polymeric OLEDs, synthetic methods can be used to tailor the emission. For example, replacing the CH in the 4 position of the quinolate ligand of Alq with a heterocyclic N leads to a 60 nm red shift in luminescence relative to Alq (62). Narrowing and shifting of the emission can also be effected through resonant cavity design. By tailoring the thickness and dielectric constants of the layers, the profile of broad emission from a device can be improved (63).

### 6.1.3. Device Stability

Stability of OLEDs has been a significant problem, since many organic materials are susceptible to oxidation. The mechanism of degradation in PPV-based devices has been shown to be related to the formation of singlet oxygen (64). Similarly, metal quinolate devices degrade quickly upon exposure to atmosphere water vapor and oxygen. Packaging devices under anaerobic conditions has been shown to extend device lifetime considerably, and devices with operating lifetimes of over 10,000 hours have been reported (49). The role of impurities in device degradation has not been fully established, and the behavior of the organic–contact interface remains

an area of intense study. The thermal properties of the organic materials also limit their ultimate lifetime. Increasing the glass-transition temperatures without lowering the carrier mobilities of organic materials is a very active area of research, which may lead to more stable devices or devices that can function well at elevated temperatures.

#### 6.1.4. Efficiency

Efficiency of a device can be reported in terms of an internal quantum efficiency (photons generated/electrons injected). The external quantum efficiency often reported is lower, since this counts only those photons that escape the device. Typically only a fraction of photons escape, due to refraction and waveguiding of light at the glass interface (65). The external efficiency can be increased through the use of shaped substrates (60).

Regardless of device design, for maximum quantum efficiency it is important to have a highly fluorescent emissive center. Many emitters are therefore highly absorbing and rigid, qualities that lead to large fluorescence. Because of spin selection rules governing recombination of the electron and hole, only one quarter of recombinations will lead to singlet excited states. The rest will result in triplet states, which are usually not efficient. This limits the internal quantum efficiency to a nominal maximum of 25%. However, other processes such as triplet-triplet annihilation may increase this value, and the question of the maximum possible efficiency is still not resolved. Though efficiencies for devices have climbed significantly in recent years, further improvements in efficiency are possible.

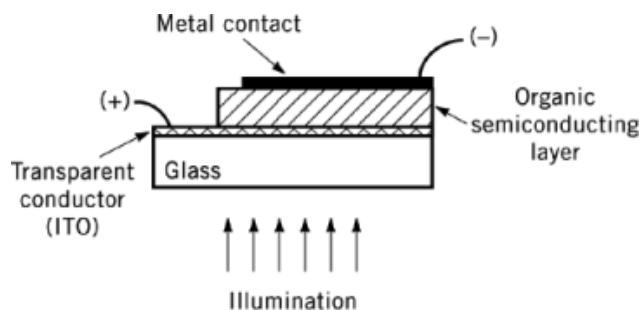
#### 6.1.5. Outlook

OLEDs in their current form meet the requirements for several low resolution applications, and with improvements in reliability, efficiency and color tuning they should soon find use in a number of display applications. One area of application will be flexible displays. Organic OLED devices (both molecular and polymer based) on polymer supports have remarkable stability even after repeated bending at sharp angles (67, 68). This high degree of substrate flexibility and device stability make these polymer-supported devices attractive for a range of applications, including portable roll-up displays and conformable displays for attachment to windows, windshields, or instrument panels. Aside from bendable devices, transparent OLEDs (TOLEDs) can be created by using a semitransparent metal cathode (69). These devices are  $>71\%$  transparent when turned off, with light emitted from both top and bottom device surfaces when voltage is applied.

There are technical problems to be overcome before OLEDs can become competitive with liquid crystal technology for use in full color, high definition displays such as computer screens. Improvements in both color saturation and reliability are needed. A review of the prospects of OLEDs for a variety of uses has been published (70). Improvements in color saturation may be realized through the use of microcavities, with layer design used to select red, green, or blue emission from a single broad-emitter material (71, 72). Recent development of stacked, independently addressable OLEDs may also lead to improvements in resolution, with three devices (R,G,B) in a vertical configuration providing minimal pixel size (73). Further improvements in the technology should lead to increasing use of OLEDs in a variety of applications.

### 6.2. Photovoltaic Devices

For many inorganic semiconductors, absorption of light can be used to create free electrons and holes. In an organic semiconducting solid, however, absorption of a photon leads to the formation of a bound electron-hole pair. Separation of this pair in an electric field can occur due to differing mobilities of the electron and hole, and this separation of the charge particles gives rise to a photovoltage (see Photovoltaic cells). This photovoltaic effect is of great interest for use in solar cells, since the conversion of light energy from the sun to electrical energy provides a nonpolluting renewable energy source. The photovoltaic effect is also of interest for photodetectors and for memory storage devices. Photocurrents are of great importance in biological systems as well, and there is interest in light-harvesting devices based on protein pigments (74).



**Fig. 10.** Typical design for single-layer photovoltaic device.

Solar cells and other photovoltaic devices have typically been based on silicon or other inorganic materials, which can provide high power conversion efficiencies (>25%). However, organic materials can also be used to generate a photovoltage. Photovoltaic effects have been studied in a wide variety of materials including solvent-cast films of Buckminsterfullerene ( $C_{60}$ ) (75) and self-assembled films of alkyl-derivatized metaloporphyrins (76). Many of these systems produce a photovoltage; however, the efficiency is lower than that found in inorganic-based devices.

#### 6.2.1. Device Structure

In both inorganic and organic materials, absorption of light generates electrons and holes, but these will recombine and lead to a loss in device efficiency unless they can be separated and made to flow through an external circuit. There are many types of junctions that are used to separate the electron and hole. In single-crystal inorganic devices, a  $p$ - $n$  junction is created by adjoining precisely doped  $p$  and  $n$ -type regions. For organic devices, a  $p$ - $n$  junction can be fabricated by sequential deposition of thin films of  $n$ -type (electron accepting) and  $p$ -type (electron donating) organic materials. Schottky junctions, formed at semiconductor-metal interfaces, are often used in simple organic photovoltaic cells. In all cases, the potential across the junction is used to sweep the photogenerated carriers toward the opposite electrodes.

A typical organic-based photovoltaic cell (Fig. 10) consists of thin films of an organic semiconducting material sandwiched between conductive surfaces, at least one of which must be transparent (such as glass-indium tin oxide). The organic layer is thin, typically ca 100 nm thick, and can be deposited by solvent evaporation or by sublimation under vacuum (77). The organic layer must be relatively thin to minimize resistance in the device. It must also be uniform and defect free (since defects can serve as traps for the charge carriers) and must be also free of pinholes which would lead to short circuiting of the device. In order to maximize efficiency, highly absorbing species are often incorporated into the device. Unlike inorganic devices, organic photovoltaic cells offer the possibility of modifying device properties such as spectral sensitivity through changing of chemical substituents of molecules in the device.

#### 6.2.2. Device Performance

Early sandwich type devices using metal-free phthalocyanines (molar absorptivities of  $\sim 10^5$ ) between gold electrodes were reported to have quantum efficiencies of 0.16% (power conversion efficiencies of 0.009%) (78). Single-dye, Schottky-type sandwich cells have been fabricated from both  $n$ -type dyes such as rhodamine B and  $p$ -type dyes such as merocyanine (79) with appropriate metal contacts. Although single-layer cells have been developed with improved efficiency compared to early devices, cells based on  $p$ - $n$  heterojunctions promise superior performance. These cells possess advantages over single-dye devices, including a broader spectral range. Heterojunction solar cells typically consist of two films of organic dyes between indium tin oxide (ITO) and metallic electrodes. To facilitate charge separation, the dyes have large differences in Fermi levels. Highly

## 20 SEMICONDUCTORS, ORGANIC

efficient organic based cells have been fabricated utilizing thermally robust phthalocyanines and perylene derivatives (16). These *p-n* type devices provide absorption throughout the visible spectrum and monochromatic internal quantum efficiencies of up to 20%.

Aside from dye-based cells, a good deal of study has been devoted to photovoltaic effects in polymer-based devices. Single-layer sandwich-type devices composed of aluminum–polyphenylenevinylene–ITO have been fabricated with solution-cast polymer layers of  $\sim 0.5\mu$ . These devices display quantum efficiencies of up to 5% (power efficiencies of 0.07%), though the efficiency decreases at high illumination levels (80). Other single-layer polymer devices fabricated with polyacetylene show similar efficiencies (81). To obtain optimum efficiency in a photovoltaic device, it is necessary to dissociate the exciton before the charges recombine to generate a photon, and a resulting loss in device efficiency. Multilayer devices consisting of separate donor and acceptor layers generate substantial improvement in device efficiency by facilitating dissociation of the electron-hole pair. In these two-layer devices, excitons that diffuse to the D-A interface are separated (the electron going to the acceptor), and the charges can then be swept on to the electrodes through their respective layers.

However, not all excitons have sufficiently long lifetimes to reach the interface before recombining. To circumvent this problem and increase device efficiency, heterostructure devices have been fabricated. In these devices, donors and acceptors are mixed together to create a network that provides many internal interfaces where charge separation can occur. Heterostructure devices made from the donor polymer poly(2-methoxy-5-(2'-ethyl-hexyloxy-*p*-phenylenevinylene) (MEH-PPV) mixed with the acceptor polymer CN-PPV (a cyano-substituted derivative of PPV) showed improved performance (82).

### 6.2.3. Outlook

Organic materials could provide much cheaper solar cells, since crystalline or epitaxially grown inorganic materials are costly. Also, deposition of organic compounds in vacuum could provide for large-area or custom shaped cells. Recent advances have greatly improved the efficiency of polymer-based solar cells, though they still suffer from a lower efficiency than inorganic-based devices. Also, the polymers suffer from photostability problems that must be overcome. However, they still could see near-term use in applications which do not require exposure to powerful light sources.

### 6.3. Transistors

The use of molecular materials for transistors is attractive because of the facile processability and low cost of organic thin films. Early organic thin-film transistors (TFTs) based on lutetium bis-phthalocyanine (83), polyacetylene (84), or polythiophene derivatives (85) as the active component were shown to have source-drain currents that could be modulated with applied gate voltage. However, performance of early devices was poor compared to inorganic-based devices, and turn-on times were slow. Mobilities for phthalocyanine devices of  $\mu = 10^{-4} \text{ cm}^2/\text{V}\cdot\text{s}$  and  $\mu = 10^{-5} \text{ cm}^2/\text{V}\cdot\text{s}$  for polythiophene devices are some four to five orders of magnitude below the mobilities for Si-based devices. Though stable field-effect transistors based on metal phthalocyanines have been developed with mobilities of  $10^{-3} \text{ cm}^2/\text{V}\cdot\text{s}$ , much of the research on organic field-effect transistors has focused on semiconducting polymeric materials. Early devices typically generated the polymer electrochemically under inert atmosphere (86) or by spincoating; devices with enhanced performance were fabricated using vacuum deposition of oligomers. Devices from  $\alpha$ -conjugated oligomers of polythiophene ( $\alpha$ -sexithienyl,  $\alpha$ -6T) showed mobility enhancement after heat treatment, with maximum  $\mu = 10^{-3} \text{ cm}^2/\text{V}\cdot\text{s}$  reported (87). These *p*-type polycrystalline thin films (thicknesses of 100–200 nm) give on/off current ratios of  $10^2$ – $10^3$ .

“All-organic” transistors based on  $\alpha$ -6T were designed with organic materials serving as the semiconductor, insulator, and support (the source and drain contacts were metallic) (88). Aside from being flexible as a result of the organic support, these devices showed very high mobilities. The reported field-effect mobility ( $4.6 \times 10^{-1}$ ) and transit times are similar to those of amorphous-silicon based transistors. The performance of these devices

was noted to be highly dependent on the nature of the semiconductor–insulator interface. Later refinement of  $\alpha$ -6T based devices has improved the ratio of source-drain currents in the on and off states, with ratios of  $>10^6$  obtained (89). Aside from the *p*-type polymer, hole transporting devices, *n*-type devices have been fabricated. In addition, devices have been developed that can function in either *n* or *p* type modes. Heterostructure devices consisting of  $C_{60}$  and  $\alpha$ -6T active layers provide hole or electron drain currents depending upon the gate bias (90). The improvements in device performance are continuing, and organic transistors are likely to become important in a number of applications ranging from displays to integrated circuits.

#### 6.4. Reproduction and Resist Materials

Organic photoreceptors have advantages over inorganic-based systems in cost and flexibility. Organic charge-transfer complexes, polymers, and dyes have found wide use in xerography (see Electrophotography). The role of the photoreceptor is to convert an optical input signal to an electrostatic map on a photoconductive surface. The photoreceptor must accept and hold a surface charge, discharging only in those areas that are exposed to illumination. Oppositely charged toner particles are then attracted to the undischarged areas of the photoconductor to create an image representing the dark regions of the original image.

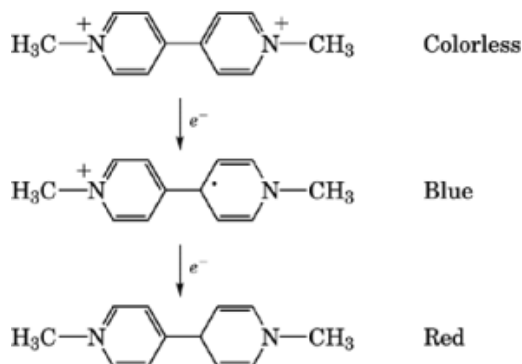
The photoreceptor must be highly optically absorbing throughout the visible region, must be stable with respect to light and chemicals such as ozone, and must be relatively insulating in the absence of illumination. The field of organic photoconducting materials has been reviewed (91, 92).

The first use of organic charge transfer complexes was of poly(*N*-vinylcarbazole) [25067-59-8] (PVK) mixed with the acceptor 2,4,7-trinitro-9-fluorenone [129-79-3] (TNF) in a 1:1 ratio (93). In this device, charge generation through absorption and charge transport both occur in a single layer. This material had good sensitivity throughout the visible region, but the carcinogenic properties of the fluorenone led to the discontinuation of its commercial use. A number of other acceptors have been used as dopants in PVK, including tetracyanoethylene, tetracyanoquinodimethane, and chloranil (94). Charge-transfer complexes from triarylamine donors and boron diketonate acceptors have also been investigated for use as photoreceptors when doped into a Lexan host (95). The use of single-layer devices has been supplanted by two-layer systems, with one layer used for charge generation and the other for charge transport. Highly absorbing organic dye molecules are typically usually used for charge-generation and doped polymers serve as transport layers.

#### 6.5. Batteries

Many  $\pi$ -conjugated polymers can be reversibly oxidized or reduced. This has led to interest in these materials for charge-storage batteries, since polymers are lightweight compared to metallic electrodes and liquid electrolytes. Research on polymer batteries has focused on the use of polymers as both the electrode and electrolyte. Typical polymer electrolytes are formed from complexes between metal-ion salts and polar polymers such as poly(ethyleneoxide). The conductivity is low at room temperature due to the low mobility of cations through the polymer-matrix, and the batteries work more efficiently when heated above the glass-transition temperature of the polymer. Advances in the development of polymer electrolytes have included polymers poly(ethylene oxide) intercalated into layered silicates (96). These solid-phase electrolytes exhibit significantly improved conductance at room temperature.

A variety of polymers have been investigated for use as electrodes, including polyacetylene and polyaniline. The stability of polymer electrodes with respect to repeated cycling has been a question. Although polyacetylene degrades after a limited number of cycles under oxidation, its performance for reduction is much better (97). Polymers for electrode applications must not only be robust with respect to air and repeated cycling, but must be easily processable, and cheap, and must provide high power–weight ratios. One efficient rechargeable system uses a thidiazole-based polymer which undergoes depolymerization as the battery is discharged, with



**Fig. 11.** Electrochromic behavior of methyl viologen.

the electrode being regenerated upon recharging (98). Improvements in polymer battery design should make polymer-based cells attractive, especially for low power applications.

## 6.6. Electrochromics

Oxidation or reduction of organic compounds often results in a color change (see Electrochromics). Materials exhibiting such changes are termed electrochromics. Typically, the organic is pale in color prior to oxidation or reduction, with intense color change upon application of a voltage as a result of new optical absorption bands. Electrochromic materials are of interest for use in displays as well as for optical shutters. An important parameter in performance of these devices is the read–write efficiency, which is the percentage of electrically generated color that can be removed by reversing the current through the device.

The divalent cation methyl viologen is highly colored in reduced form and is used as an electrochromic in solution cells (Fig. 11).

Other solution-based electrochromic systems have been based on TCNQ, which is soluble in organic solvents such as acetonitrile. One-electron reduction forms the highly colored  $\text{TCNQ}^-$  anion, which absorbs throughout the visible region. Polymeric derivatives of TCNQ have been chemically attached to electrode surfaces to generate reversible electrochromic systems (99). Tethering the polymer to the electrode surface prevents diffusion of species away from the electrode surface and results in improved read–write efficiencies. Other organic acceptors such as *o*-chloranil (3,4,5,6-tetrachlorobenzoquinone) have also been used in electrochromic cells, demonstrating excellent stability and highly colored radical forms.

Tetrathiafulvalene (TTF) has also been used in electrochromic devices. TTF-based polymers spin-coated onto transparent electrode surfaces form stable thin films with reproducible electrochromic properties (100). The slow response of these devices has been attributed to the rate of ion movement through the polymer matrix.

The use of polymeric materials for electrochromic displays is especially promising. A number of conjugated polymer systems can be used as electrochromics, with insulating and doped forms of the polymer exhibiting different absorption spectra (101, 102). Electrochemical oxidation of aniline results in thin films of polyaniline, which can exist in various redox states. Successive oxidations cause reversible color changes from transparent to yellow–green to deep blue–black (103). Polythiophene can also be electrochemically generated from the monomer. Though polythiophene electrochromic films suffer a loss in read–write efficiency after a large number of read–write cycles, derivatives of polythiophene have found use as electrochromes in a number of devices including display (104) and memory (105) devices. The colors in the oxidized and reduced forms of these systems depend upon the nature of the substituents on the monomer unit.

### 6.7. Switches and Sensors

The use of conducting polymers has been shown to be promising for chemical sensor technology, with molecular recognition leading to changes in conductivity of the polymer. One approach utilizes polythiophene derivatives which undergo ion-specific conformational changes, resulting in conductivity reductions upon sensing (106). Switching phenomena in charge-transfer complexes has also been observed. Thin films of metal-organic charge-transfer complexes such as Cu-TCNQ can be switched between low and high conductivity states with application of a suitable field. Conduction in the high conductivity state has been associated with channel formation in the material (107). One design for optoelectronic gates incorporates a dye molecule as the absorbing chromophore with a series of linked metalloporphyrins serving as a molecular wire. Switching is observed as a result of the change in the porphyrin energy levels (and thus the conduction in the wire) upon reversible oxidation at a designated site (108). Polymeric systems also show promise as temperature sensors, since thin films of doped polymers such as polyacetylene exhibit temperature dependent color changes.

## BIBLIOGRAPHY

"Semiconductors, Organic," in *ECT* 3rd ed., Vol. 20, pp. 674-698, by Robert C. Haddon, Martin L. Kaplan, Fred Wudl, Bell Laboratories.

### Cited Publications

1. F. Gutman, H. Keyzer, L. Lyons, and R. B. Samoano, *Organic Semiconductors*, part B, Robert E. Kreiger Publishing Co., Malabar, Fla., 1983, 399-412.
2. Peierls, *Quantum Theory of Solids*, Oxford University Press, 1972.
3. M. H. Whangbo, in J. S. Miller, ed., *Extended Linear Chain Compounds*, Plenum Press, New York, 1982, p. 127.
4. R. S. Mulliken and W. B. Person, *Molecular Complexes*, John Wiley & Sons, Inc., New York, 1969.
5. Z. Soos, *J. Chem. Ed.* **55**(9), 549 (1978).
6. Ref. 1, p. 400.
7. D. Jérôme, A. Mazaud, M. Ribault, and K. Bechgaard, *J. Phys. Lett (Orsay)* **41**, L95 (1980).
8. U. Geiser, J. A. Schlueter, H. H. Wang, A. M. Kini, J. M. Williams, P. P. She, H. I. Zakowicz, M. L. VanZile, and J. D. Dudek, *J. Am. Chem. Soc.* **118**, 9996 (1996).
9. J. Kanicki, in T. A. Skotheim, ed., *Handbook of Conducting Polymers*, Vol. **1**, Marcel Dekker, New York, 1986, 544-660.
10. W. P. Su and co-workers, *Phys. Rev. Lett.* **42**, 1698 (1979).
11. A. O. Patil, A. J. Heeger, and F. Wudl, *Chem. Rev.* **88**, 183 (1988).
12. J. Kanicki, S. Boué, and E. Vander Donckt, *Thin Solid Films* **92**, 243 (1982).
13. H. Eckhardt, L. W. Shacklette, K. Y. Jen, and R. L. Elsenbaumer, *J. Chem. Phys.* **91**(2), 1303 (1989).
14. K. Bechgaard, in W. E. Hatfield, ed., *Molecular Metals*, Plenum Press, New York, 1979, p. 1.
15. B. H. Cumpston, K. F. Jensen, F. Klavetter, E. G. J. Staring, and R. C. J. E. Demandt, *Mat. Res. Soc. Proc.* **413**, 35 (1996).
16. J. B. Whitlock, P. Panayotatos, G. D. Sharma, M. D. Cox, R. R. Sauers, and G. B. Bird, *Optical Eng.* **32**(8), 1921 (1993).
17. Ref. 1, p. 242.
18. H. R. Allcock and F. W. Lampe, *Contemporary Polymer Chemistry*, 2nd ed., Prentice-Hall, Englewood Cliffs, N.J., 1990.
19. F. Garnier, A. Yassar, R. Hajlaoui, G. Horowitz, F. Deloffre, B. Servet, S. Ries, and P. Alnot, *J. Am. Chem. Soc.* **115**, 8716 (1993).
20. I. Rubinstein, J. Ripshon, E. Sabatani, A. Redondo, and S. Gottesfeld, *J. Am. Chem. Soc.* **112**, 6315 (1990).
21. F. Wudl, R. O. Angus, Jr., F. L. Lu, P. M. Allemand, D. J. Vachon, M. Nowak, Z. X. Liu, and A. J. Heeger, *J. Am. Chem. Soc.* **109**, 3677 (1987).
22. R. D. McCullough, M. D. Mays, A. B. Bailey, and D. O. Cowan, *Synth. Met.* **27**, B487-B491 (1988).
23. D. S. Acker and W. R. Hertler, *J. Am. Chem. Soc.* **84**, 3370 (1962).
24. L. R. Melby, R. J. Harder, W. R. Hertler, W. Mahler, P. E. Benson, and W. E. Mochel, *J. Am. Chem. Soc.* **84**, 3374 (1962).

25. P. Bando, N. Martin, J. Segura, C. Seoane, E. Orti, P. Viruela, and R. Viruela, *J. Org. Chem.* **59**, 4618–4629 (1994).
26. R. M. Metzger, in R. R. Birge, ed., *Molecular and Biomolecular Electronics*, American Chemical Society, Washington, D.C., 1994, p. 91.
27. T. Ito, H. Shirakawa, and S. Ikeda, *J. Polym. Sci., Polym. Chem. Ed.* **12**, 11 (1974).
28. J. H. Edwards and W. J. Feast, *Polym. J.* **21**, 595 (1980).
29. T. M. Swager and R. H. Grubbs, *J. Am. Chem. Soc.* **111**, 4413–4422 (1989).
30. F. L. Klavetter and R. H. Grubbs, *J. Am. Chem. Soc.* **110**, 7807 (1988).
31. J. Yue and A. J. Epstein, *J. Am. Chem. Soc.* **112**, 2800–2801 (1990).
32. S. Chen and G. Hwand, *J. Am. Chem. Soc.* **117**, 10055–10062 (1995).
33. D. Fichou, G. Horowitz, B. Xu, and F. Garnier, *Synth. Met.* **89**, 243 (1990).
34. M. Corn, ed., *Handbook of Hazardous Materials*, Academic Press, 1993 p. 650.
35. M. Sittig, ed., *Handbook of Toxic and Hazardous Chemicals and Carcinogens*, 2nd ed., Noyes Publications, Park Ridge, N.J., 1985.
36. J. Dresner, *RCA Rev.* **30**, 322 (1969).
37. W. Helfrich and W. G. Schneidere, *Phys. Rev. Lett.* **14**, 229 (1965).
38. D. F. Williams and M. Schadt, *Proc. IEEE* **58**, 476 (1970).
39. C. W. Tang and S. A. VanSlyke, *Appl. Phys. Lett.* **51**, 913 (1987).
40. C. W. Tang, S. A. VanSlyke, and C. A. Chen, *J. Appl. Phys.* **65**, 3610 (1989).
41. C. Hosokawa, H. Higashi, H. Nakamura, and T. Kusumoto, *Appl. Phys. Lett.* **67**, 3853–3855 (1995).
42. J. Kido and K. Nagai, *JALCOM* **192**, 30–33 (1993).
43. Y. Hamada, T. Sano, M. Fujita, T. Fujii, Y. Nishio, and K. Shibata, *Jpn. J. Appl. Phys.* **32**, 514–515 (1993).
44. M. Takeuchi, H. Masui, I. Kikuma, M. Masui, T. Muranoi, and T. Wada, *Jpn. J. Appl. Phys.* **31**, 498–500 (1992).
45. C. Adachi, T. Tsutsui, and S. Saito, *Appl. Phys. Lett.* **56**, 799–801 (1990).
46. C. Hosokawa, H. Higashi, H. Nakamura, and T. Kusumoto, *Appl. Phys. Lett.* **67**, 3853–3855 (1995).
47. P. E. Burrows, Z. Shen, V. Bulovic, D. M. McCarty, S. R. Forrest, J. A. Cronin, and M. E. Thompson, *J. Appl. Phys.* **79**, 91–8005 (1996).
48. Y. Hamada, T. Sano, M. Fujita, T. Fujii, Y. Nishio, and K. Shibata, *Chem. Lett.*, 905–906 (1993).
49. S. A. VanSlyke, C. H. Chen, and C. W. Tang, *Appl. Phys. Lett.* **69**, 2160 (1996).
50. G. Gustaffason, G. M. Treacy, Y. Cao, F. Klavetter, N. Colaneri, and A. J. Heeger, *Synth. Met.* **57**, 4123 (1993).
51. V. Bulovic, G. Gu, P. E. Burrows, S. R. Forrest, and M. E. Thompson, *Nature* **380**, 29 (1996).
52. V. Bulovic, G. Gu, P. E. Burrows, S. R. Forrest, and M. E. Thompson, *Appl. Phys. Lett.* **68**, 2606–2608 (1996).
53. G. E. Johnson, K. M. McGrane, and M. Stolka, *Pure Appl. Chem.* **67**, 175–182 (1995).
54. P. E. Burrows, S. R. Forrest, S. P. Sibley, and M. E. Thompson, *Appl. Phys. Lett.* **69**, 2959 (1996).
55. J. Kido, M. Kimura, and K. Kagai, *Science* **267**, 1332 (1995).
56. J. Tian, C. C. Wu, M. E. Thompson, J. C. Sturm, R. A. Register, M. J. Marsella, and T. M. Swager, *Adv. Mater.* **7**, 395–398 (1995).
57. J. Pommerehne, H. Vestweber, W. Guss, R. F. Mahrt, H. Bassler, M. Porsch, and J. Daub, *Adv. Mater.* **7**, 551–554 (1995).
58. C. Zhang, H. von Seggern, B. Kraabel, H.-W. Schmidt, and A. J. Heeger, *Synth. Met.* **72**, 185–188 (1995).
59. J. Kido, M. Kohda, K. Okuyama, and K. Nagai, *Appl. Phys. Lett.* **61**, 761–763 (1992).
60. C. Zhang, H. von Seggern, K. Pakbaz, B. Kraabel, H.-W. Schmidt, and A. J. Heeger, *Synth. Met.* **62**, 35–40 (1994).
61. J. Kido, H. Shionoya, and K. Magai, *Appl. Phys. Lett.* **67**, 2281–2283 (1995).
62. Z. Shen, P. Burrows, D. Z. Garguzov, M. McCarty, M. E. Thompson, and S. R. Forrest, *J. Appl. Phys.* **35**, L401 (1996).
63. N. Takada, T. Tsutsui, and S. Saito, *Appl. Phys. Lett.* **63**, 2022 (1993).
64. R. D. Scurlock, B. Wang, P. R. Ogilby, J. R. Sheats, and R. L. Clough, *J. Am. Chem. Soc.* **117**, 10194–10202 (1995).
65. N. C. Greenham, R. H. Friend, and D. C. Bradley, *Adv. Mater.* **6**, 491 (1994).
66. G. Gu, D. Z. Garbazov, P. E. Burrows, S. Venkatesh, S. R. Forrest, and M. E. Thompson, *Optics Letters* **22**, 397 (1997).
67. G. Gustafsson, G. M. Treacy, Y. Cao, F. Klavetter, N. Colaneri, and A. J. Heeger, *Synth. Met.* **55–57**, 4123 (1993).
68. G. Gu, P. E. Burrows, S. Venkatesh, S. R. Forrest, and M. E. Thompson, *Optics Letters* **22**, 172 (1997).
69. V. Bulovic, G. Gu, P. E. Burrows, S. R. Forrest, and M. E. Thompson, *Nature* **380**, 29 (1996).
70. L. J. Rothberg and A. J. Lovinger, *J. Mater. Res.* **11**(12), 3174 (1996).
71. A. Dodabalapur, L. J. Rothberg, T. M. Miller, and E. W. Kwock, *Appl. Phys. Lett.* **64**, 19 (1994).



72. A. Dodabalapur, L. J. Rothberg, and T. M. Miller, *Electronics Lett.* **30**, 1000 (1994).
73. Z. Shen, P. E. Burrows, V. Bulovic, S. R. Forrest, and M. E. Thompson, *Science* **276**, 2009 (1997).
74. F. T. Hong, in Ref. 26, p. 554.
75. C. H. Lee, G. Yu, D. Moses, A. J. Heeger, and V. I. Srdanov, *Appl. Phys. Lett.* **65**, 6, 664 (1994).
76. C.-Y. Liu, H.-L. Pan, H. Tang, M. A. Fox, and A. J. Bard, *J. Phys. Chem.* **99**, 7632 (1995).
77. R. N. Marks, R. Zamboni, and C. Taliani, *Mat. Res. Soc. Symp. Proc.* **247**, 814 (1996).
78. K. J. Hall, J. S. Bonham, and L. E. Lyons, *Aust. J. Chem.* **31**, 1661 (1978).
79. D. Wöhrle and D. Meissner, *Adv. Mat.* **3**, 129 (1991).
80. H. Antoniadis, B. R. Hsieh, M. A. Abkowitz, S. A. Jenekhe, and M. Stolka, *Synth. Met.* **62**, 265–271 (1994).
81. J. Kanicki, in T. A. Skotheim, ed., *Handbook of Conducting Polymers*, Vol. **1**, Marcel Dekker, New York, 1986, p. 543.
82. J. J. M. Halls, C. A. Walsh, N. C. Greenham, E. A. Marseglia, R. H. Friend, S. C. Moratti, and A. B. Holmes, *Nature* **376**, 498 (1995).
83. R. Madru, G. Guillaud, M. Al Sadoun, M. Maitrot, J.-J. André, J. Simon, and R. Even, *Chem. Phys. Lett.* **145**(4), 343 (1988).
84. F. Ebisawa, T. Kurosawa, and S. Nara, *J. Appl. Phys.* **54**, 3255 (1983).
85. A. Assadi, C. Svensson, M. Willander, and O. Inganäs, *Appl. Phys. Lett.* **53**, 195 (1988).
86. A. Tsumura, H. Koezuka, and T. Ando, *Synth. Met.* **25**, 11 (1988).
87. G. Horowitz, D. Fichou, X. Peng, Z. Xu, and F. Garnier, *Solid State Comm.* **72**, 381 (1989).
88. F. Garnier, G. Horowitz, X. Peng, and D. Fichou, *Adv. Mat.* **2**, 592 (1990).
89. A. Dodabalapur, L. Torsi, and H. E. Katz, *Science* **268**, 270 (1995).
90. A. Dodabalapur, H. E. Katz, L. Torsi, and R. C. Haddon, *Science* **269**, 1560 (1995).
91. P. M. Borsenberger and D. S. Weiss, in A. S. Diamond, ed., *Handbook of Imaging Materials*, Marcel-Dekker, New York, 1991, p. 379.
92. P. M. Borsenberger and D. S. Weiss, *Organic Photoreceptors for Imaging Systems*, Marcel Dekker, New York, 1993.
93. W. D. Gill, *J. Appl. Phys.* **43**, 5033 (1972).
94. H. Meier, W. Albrecht, E. Zimmerhackl, N. Geheeb, and U. Tschirwitz, *Polym. Bull.* **7**, 505 (1982).
95. T. E. Goliber and J. H. Perlstein, *J. Chem. Phys.* **80**, 4162 (1984).
96. S. Wong, S. Vasudevan, R. A. Vaia, E. P. Gianelis, and D. B. Zax, *J. Am. Chem. Soc.* **117**, 7568 (1995).
97. R. B. Kaner and A. G. McDiarmid, *Synth. Met.* **14**, 3 (1986).
98. C. Vaughan, *New Scientist*, **31**, 36 (1990).
99. R. W. Day, G. Inzelt, J. F. Kinstle, and J. Q. Chambers, *J. Am. Chem. Soc.* **104**, 6804 (1982).
100. F. B. Kaufman, A. H. Schroeder, E. M. Engler, S. R. Kramer, and J. Q. Chambers, *J. Am. Chem. Soc.* **102**, 483 (1990).
101. M. Gazar, in T. A. Skotheim, ed., *Handbook of Conducting Polymers*, Marcel Dekker, New York, 1986, Chapt. 19.
102. P. M. S. Monk, R. J. Mortimer, and D. R. Rosseinski, *Electrochromism: Fundamentals and Applications*, VCH Publishing Co., Weinheim, 1984.
103. T. Kobayashi, H. Yonehama, and H. Tamura, *J. Electroanal. Chem.* **161**, 419 (1984).
104. E. M. Genies, M. Lapowski, C. Santier, and E. Viel, *Synth. Met.* **18**, 631 (1987).
105. K. Yoshino, R. Sugimoto, J. G. Rose, and W. F. Schmidt, *Jpn. J. App. Phys.* **24**, L33 (1985).
106. T. M. Swager, M. J. Marsella, Q. Zhou, and R. J. Newland, *Mat. Res. Soc. Symp. Proc.* **413**, 407 (1996).
107. H. Duan, M. D. Mays, D. O. Cowan, and J. Kruger, *Synth. Met.* **28**, C675–680 (1989).
108. R. W. Wagner, J. S. Lindsey, J. Seth, V. Palaniappan, and D. F. Bocian, *J. Am. Chem. Soc.* **118**, 3996 (1996).

SCOTT P. SIBLEY  
Goucher College

## Related Articles

Photovoltaic cells; Electrochromics; Sensors